ELSEVIER

Normalization of Sun/View Angle Effects Using Spectral Albedo-Based Vegetation Indices

J. Qi, M. S. Moran,* F. Cabot,† and G. Dedieu†*

Current vegetation indices are normally computed with directional spectral reflectances and are subjected to many external perturbations such as soil background variations, atmospheric conditions, geometric registration, and especially sensor viewing geometry. Subsequent use of these indices to estimate vegetation amounts would result in substantial uncertainties. To reduce the uncertainties due to sun / view angle variations, spectral albedos, which are integrated reflectance values over a hemisphere of the surface within the specific spectral waveband, were derived from multidirectional measurements and bidirectional reflectance distribution function (BRDF) models and were subsequently used in vegetation index computations. The albedo-based vegetation indices were then compared with those computed with spectral reflectances using ground-, aircraft-, and satellite-based remote sensing measurements over harvested alfalfa, full-cover cotton canopy, pecan orchards, and bare soil surfaces. The results showed that spectral albedo-based vegetation indices were independent of view angles while the spectral reflectance vegetation indices varied substantially with sensor viewing geometry. Therefore, the view angle effects on spectral vegetation indices can be normalized, and the sun angle effects can be further reduced with a limited number of multidirectional measurements and BRDF models.

INTRODUCTION

To monitor vegetation status at regional and global scale for environmental change studies, remote sensors with large spatial coverage and high temporal frequency have been launched on satellites and space aircraft. Examples are the Advanced Very High Resolution Radiometer (AVHRR) on the National Oceanic and Atmospheric Administration (NOAA) satellite series and the proposed Moderate-resolution Imaging Spectrometer (MODIS) to be on board the earth observing system (EOS) platforms. These sensors have the ability to sense the entire Earth on a daily basis because of their large field of view (FOV). However, the large FOV also results in some problems associated with the bidirectional effects due to sun / view angle differences. Consequently, it is very difficult to compare remote sensing data acquired at different times and locations in quantitative analysis. In order to efficiently utilize high temporal resolution and large spatial scale remote sensing data, the sun / view angle effects must be understood and quantified / normalized.

Studies have been made to address the bidirectional effects due to sun position and sensor viewing geometry (Holben and Kimes, 1986; Jackson et al., 1990; Qi et al., 1994a; Mouginis-Mark et al., 1994; Schaaf and Strahler, 1994). These studies showed, in general, that surface anisotropic properties exerted substantial effects on the bidirectional reflectance measurements and required the necessity of correction / normalization of the sun / view angle effects for quantitative analysis of remotely sensed data. More specifically, the results of these studies showed that 1) the bidirectional effects were vegetation type dependent due to shadowing and multiple scattering effects and, therefore, were difficult to quantify and 2) the sun / view angle effects were coupled with those of atmosphere and spatial scales effects. Most of these studies, however, were done in reflectance domain and the results varied with spectral wavelength. When vegetation indices (mathematical transformation of spectral reflectances to enhance vegetation signals) were computed, the bidirectional effects could be reduced (Gutman, 1991; Huete et al., 1992), but could also be worsened (Cihlar et al., 1994; Qi et al., 1994b).

*USDA-ARS Water Conservation Laboratory, Phoenix
†LERTS, Toulouse, France

Address correspondence to Jiaguo Qi, Water Conservation Lab., USDA-ARS, 4331 East Broadway Rd., Phoenix, AZ 85040.
Received 26 May 1994; revised 10 February 1995.

REMOTE SENS. ENVIRON. 52:207–217 (1995)

655 Avenue of the Americas, New York, NY 10010

0034-4257 / 95 / $9.50
SSDI 0034-4257(95)00034-X

Spectral albedo (α) is invariant with respect to the sensor viewing geometry, because it is defined as the hemispherical reflectance of the surface within the specific spectral waveband. Consequently, this physical measure would be independent of view angle and can be used to compute vegetation indices. However, to obtain spectral albedo, simultaneous reflectance measurements in all possible viewing directions are required. In practice, no such remote sensing system is capable of acquiring simultaneous multidirectional measurements, and consequently the spectral albedo calculation seems impossible from direct measurements. One approach is through modeling. Several bidirectional reflectance distribution function (BRDF) models exist to predict the bidirectional reflectance properties (Verhoef, 1984; Deering et al., 1990; Verstraete et al., 1990; Strahler and Jupp, 1991; Asrar and Myneni, 1991; Qin, 1993; Strahler, 1994; Liang and Strahler, 1994; Albuelgasim and Strahler, 1994). Most BRDF models require a knowledge about surface physical parameters such as leaf area index (LAI), single scattering albedo, leaf angle distribution, phase functions, canopy transmittance, or some empirical parameters. Since these parameters are usually not available by remote sensing means, it is difficult to use these BRDF models solely with remote sensing measurements. With a limited number of multidirectional measurements, however, these models can be inverted and spectral albedos can be calculated. This study computes vegetation indices from spectral albedos computed from multidirectional reflectance measurements and BRDF models.

MATERIALS AND METHODOLOGY

Experiments

To address the bidirectional effects on surface reflectance measurements, an experiment was conducted at the Maricopa Agricultural Center near Phoenix, Arizona on 7 and 8 September 1991. Two SPOT satellite images were acquired with view angles of +25° and −09°, where the negative sign (−) indicates that the sensor was in the same direction as the sun and the positive sign (+) was the opposite. The Advanced Solid-state Array Spectroradiometer (ASAS) was flown on NASA's C-130 aircraft to obtain images in 29 spectral bands (band centers ranged from 465 nm to 871 nm at 15-nm increments with 15-nm spectral resolution) at viewing angles ranging from −45° to +45° on both days. The C-130 was flown at 5000 m and 2000 m above the ground, resulting in a spatial resolution of 5 m and 2 m, respectively. A coincident low-altitude aircraft was also used to carry an Exotech radiometer with four spectral filters at an altitude of 150 m above ground, resulting in a spatial resolution of 40 m. The spectral filters of the Exotech radiometer included the first band of Landsat

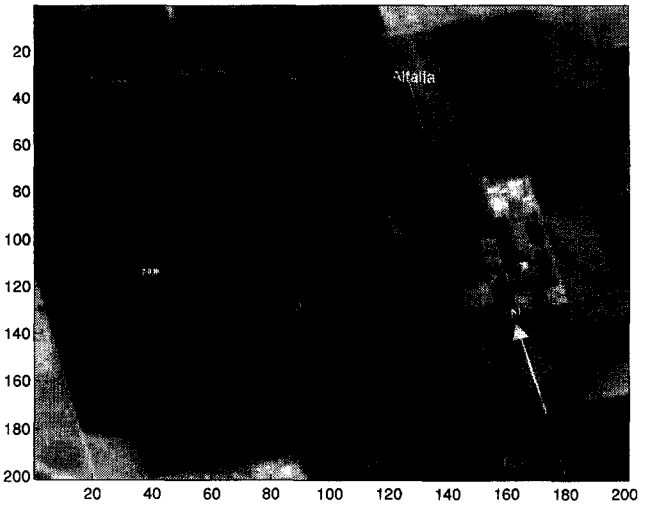

Figure 1. A SPOT image (XS1) of Maricopa Farm and the four selected study sites. The image was acquired on 7 September 1991.

Thematic Mapper (TM1) and three spectral bands of the high resolution visible (HRV) sensors on the SPOT satellite (XS1, XS2, and XS3). The radiometer was mounted in such a way that it could be turned at different view angles (40°, 30°, 20°, 0°). By changing flight direction, measurements of a total of seven view angles (±40°, ±30°, ±20°, 0°) were obtained.

The study sites (Fig. 1) included a recently harvested alfalfa field (<10%), a full cover-cotton canopy (100%), a pecan orchard canopy (60–80%), and a bare soil field (0%). The soil background conditions of the alfalfa, cotton, and soil fields were dry on both days while that of pecan orchards was wet on the first day and drier on the second day, but no quantitative soil moisture measurements were made. There was no green matter present in the alfalfa field, but some plant litter was observed. The density of pecan trees varied throughout the whole field [by randomly sampling within the whole pecan orchard field, the measured LAI varied from 0.87 to 2.48 (m^2/m^2)], but the selected site had an LAI of approximately 1.06 (m^2/m^2). The cotton field was uniform and the LAI was about 4 (m^2/m^2). The weather was clear with little haze. More details about this data set are provided by Moran et al. (1994).

Data Processing

Both ASAS and SPOT data were first calibrated/converted into surface reflectances and then were atmospherically corrected. The SPOT data were corrected with a simplified method for atmospheric correction (SMAC) by Rahman and Dedieu (1994) and the parameters used in the atmospheric corrections are listed in Table 1. For the ASAS data corrections, first we used the 5S radiative transfer code (Tanré et al., 1990) with the parameters given in Table 1 to compute the gaseous

Table 1. The Parameters Used in the Atmospheric Correction Procedures

DOY[a]	*Bands*[b]	*Water Vapor* (g/cm^2)	*Ozone Content* (g/cm^2)	*Aerosol Optical Thickness*	*Pressure* (*mbars*)
250	XS1	2.5	0.28	0.113	972.4
250	XS2	2.5	0.28	0.113	972.4
250	XS3	2.5	0.28	0.113	972.4
251	XS1	2.32	0.28	0.108	972.4
251	XS2	2.32	0.28	0.108	972.4
251	XS3	2.32	0.28	0.108	972.4

[a] DOY = day of yaer.
[b] Spectral band notations refer to the SPOT high resolution visible bands.

absorption in the ASAS spectral wavebands. In the second step, we used a new version of the Herman and Browning (1965) radiative transfer algorithm to create a lookup table (radiance vs. reflectance). Finally, the ASAS digital number was converted into radiance and multiplied by the gaseous absorption coefficients before the lookup table was used to obtain surface reflectance. For easy comparison of the data at different spatial resolutions, an area of approximately the same size (~ 120 m $\times$ 40 m) at each study site was extracted from these three data sets (Fig. 1). In order to compare data of different spectral resolutions, the extracted ASAS data were integrated into the same spectral bandwidth as those of XS1, XS2, and XS3 of the SPOT HRV sensor. This allowed a direct comparison of the three data sets, although they originally differed in both spectral and spatial resolutions.

Selected BRDF Model

In this study, we selected a semiempirical model proposed by Rahman et al. (1993a,b):

$$\rho_s(\theta_1,\phi_1,\theta_2,\phi_2) = \rho_0 \frac{\cos^{k-1}\theta_1 \cos^{k-1}\theta_2}{(\cos\theta_1 + \cos\theta_2)^{1-k}} F(g)[1 + R(G)], \quad (1)$$

where

$$F(g) = \frac{1-\Theta^2}{[1+\Theta^2 - 2\Theta\cos(\pi - g)]^{3/2}}, \quad (2)$$

$$R(G) = \frac{1-\rho_0}{1+G}, \quad (3)$$

$$G = \sqrt{\tan^2\theta_1 + \tan^2\theta_2 - 2\tan\theta_1\tan\theta_2\cos(\phi_2 - \phi_1)}, \quad (4)$$

$$\cos g = \cos\theta_1\cos\theta_2 + \sin\theta_1\sin\theta_2\cos(\phi_2 - \phi_1). \quad (5)$$

where θ_1 and θ_2 are solar and sensor zenith angles, respectively, and ϕ_1 and ϕ_2 the corresponding azimuth angles. This model was simple and required three input parameters (ρ_0, k, and Θ). The first parameter, ρ_0, is an arbitrary parameter that characterizes the intensity of surface reflectance. The constraint of its value is $0 \leqslant \rho_0 \leqslant 1$. The second parameter, k ($0 \leqslant k \leqslant 1$), is an indicator of the vegetation anisotropy. When $k = 1$, the surface anisotropy characteristics would be controlled solely by the third parameter Θ ($-1 \leqslant \Theta \leqslant +1$). The Θ parameter controls the relative contributions of the forward scattering ($0 \leqslant \Theta \leqslant +1$), and backscattering ($-1 \leqslant \Theta \leqslant 0$), therefore, is an indicator of the vegetation structures. All three of these parameters are not directly measurable because of the way they were defined (Rahman et al., 1993a,b), and there is no one-to-one relationship with any surface physical parameters. Other existing BRDF models could be used for the purpose of this study. However, a general study on the validity of existing BRDF models, using ground and airborne remote sensing data (Cabot et al., 1994), indicated that Rahman's model was as good as other more-complex BRDF models in predicting reflectances and it is simple and easy for inversion. In Figure 2, the predicted reflectances with this model were compared with the measurements using the aircraft measurements as a demonstration. The predicted reflectances were very close to the measurements with a linear coefficient of 0.998. Therefore, we selected this model for spectral albedo calculations, which were then used in vegetation index computations.

Albedos

To compute vegetation indices (VI) from spectral albedos, multidirectional measurements were first converted

Figure 2. Predicted reflectances in SPOT spectral bands versus the measurements. The prediction was made with a BRDF model by Rahman et al. (1993a,b) to demonstrate the validity of the model for the data set used.

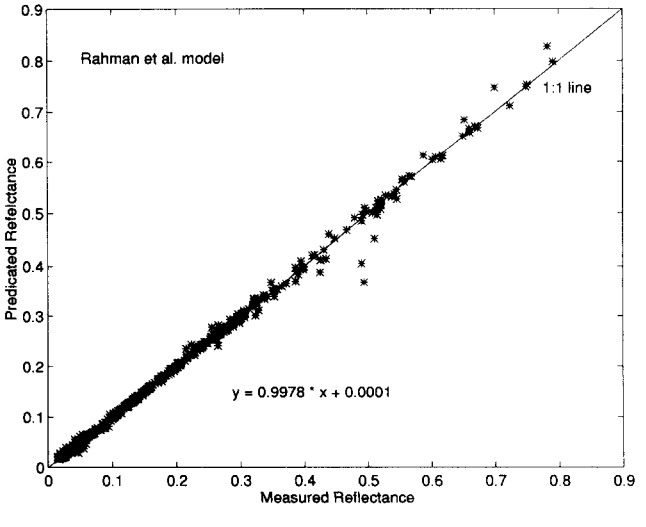

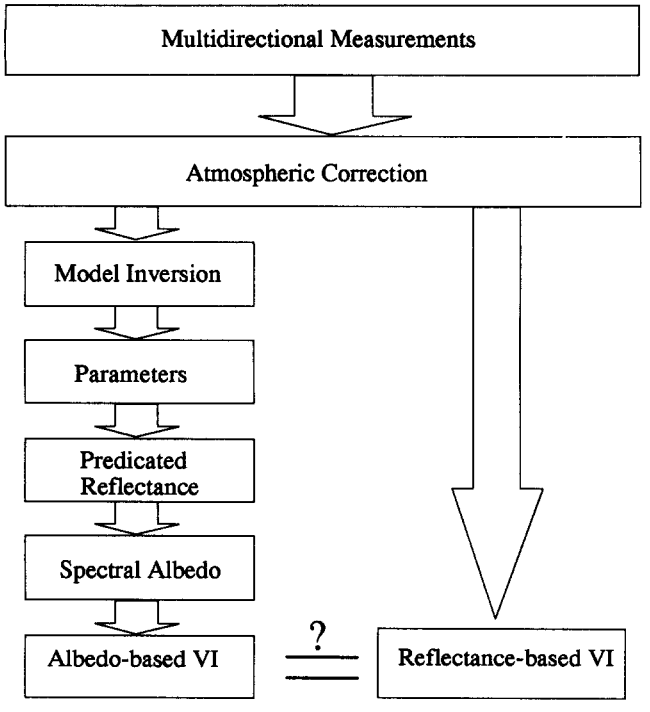

Figure 3. A flow chart of the data processing and the algorithm for albedo-based vegetation index computations.

into reflectances and then were corrected for atmospheric effects (Fig. 3). The limited number of corrected reflectances was then used in model inversion. The inversion resulted in a set of parameters (ρ_0, k, Θ), which was in turn used in direct simulations to generate multidirectional reflectances (ρ). Spectral albedos (α) were then computed using the Gauss Legendre integration algorithm over a 16×16 grid in relative azimuth difference (φ) and view zenith (θ_v) coordinates:

$$\alpha(\theta_s,\lambda) = \sum_{i=1}^{16}\sum_{j=1}^{16} v^i v^j \rho(\theta_s,\lambda,\theta_v^i,\varphi^j), \quad (6)$$

where v^i and v^j were the weights applied for each coordinate θ^i and φ^j. The spectral albedo (α) is a function of solar zenith angle (θ_s) and spectral wavelength (λ). In the final step, vegetation indices were calculated with the computed spectral albedos. The vegetation indices computed with spectral albedos were referred to as albedo-based VI while those with spectral reflectances were referred to as reflectance-based VI hereafter.

RESULTS

Reflectances and Reflectance-Based NDVI

The spectral signatures of the four selected targets are shown in Figure 4 as a function of view angle and wavelength. The bidirectional properties, especially in the near-infrared (NIR) regions, could be seen. These bidirectional effects can be enhanced when translated into vegetation indices (Qi et al., 1994a). The alfalfa site (Fig. 4a) bidirectional reflectance properties were similar to those of the bare soil site (Fig. 4b), slightly increasing with the sensor view angles. The similarity between these two study sites was due to the fact that both sites were flat surfaces and there was little to none green matter present. Nevertheless, in spite of being such flat surfaces with no green vegetation, bidirectional effects on the reflectance measurements were still evident. The large variations in reflectances found at the pecan site (Fig. 4c) were most likely due to the shadows cast by large tree trunks (bales) and leaves. The spectral reflectances of the cotton site (Fig. 4d), a full-cover canopy, also demonstrated substantial view angle effects. The large reflectance variations with view angle at the longer wavelengths may have been due to the atmospheric effects and more multiple scattering inside the canopy. Nevertheless, the bidirectional effects on the spectral reflectances of the four selected study sites were apparent and suggested that sun / view angle influences must be taken into account when utilizing off-nadir remote sensing measurements.

The bidirectional effects observed in the reflectances were also inherent in the normalized difference vegetation index (NDVI) as depicted in Figure 5. The NDVI values were calculated from the ASAS data after being integrated to the same spectral resolution as the SPOT HRV sensor. The solar zenith angles (S_z) were indicated by numbers while the viewing directions were labeled either in the principal plane (pp), orthogonal (orth) to the principal plane, or in the SPOT satellite scanning directions. All study sites showed view angle effects and a dependency on the solar zenith angles. When the sensor viewing direction was aligned either in the SPOT or in the orthogonal directions, the view angle effects were less apparent. This was due to the fact that, in the orthogonal direction (SPOT direction was also close to the orthogonal at the time of measurement), the shadowing effects were symmetric about the principal plane. The magnitudes of the sun / view angle effects were also target-dependent; the bidirectional properties of the NDVI differed among study sites. It is difficult, therefore, to correct bidirectional effects from a practical point of view. In general, the solar zenith angles altered the absolute NDVI values while the sensor view direction controlled the shapes of the NDVI values. This complexity of the NDVI variations with sun / view angles suggests that the normalization of the bidirectional effects is not possible using the reflectance-based NDVI, particularly in the principal plane with changing view and sun angles.

Spectral Albedos and Corresponding NDVI

The spectral albedo of the selected targets are depicted in Figure 6 using the ASAS data integrated to XS1 (solid

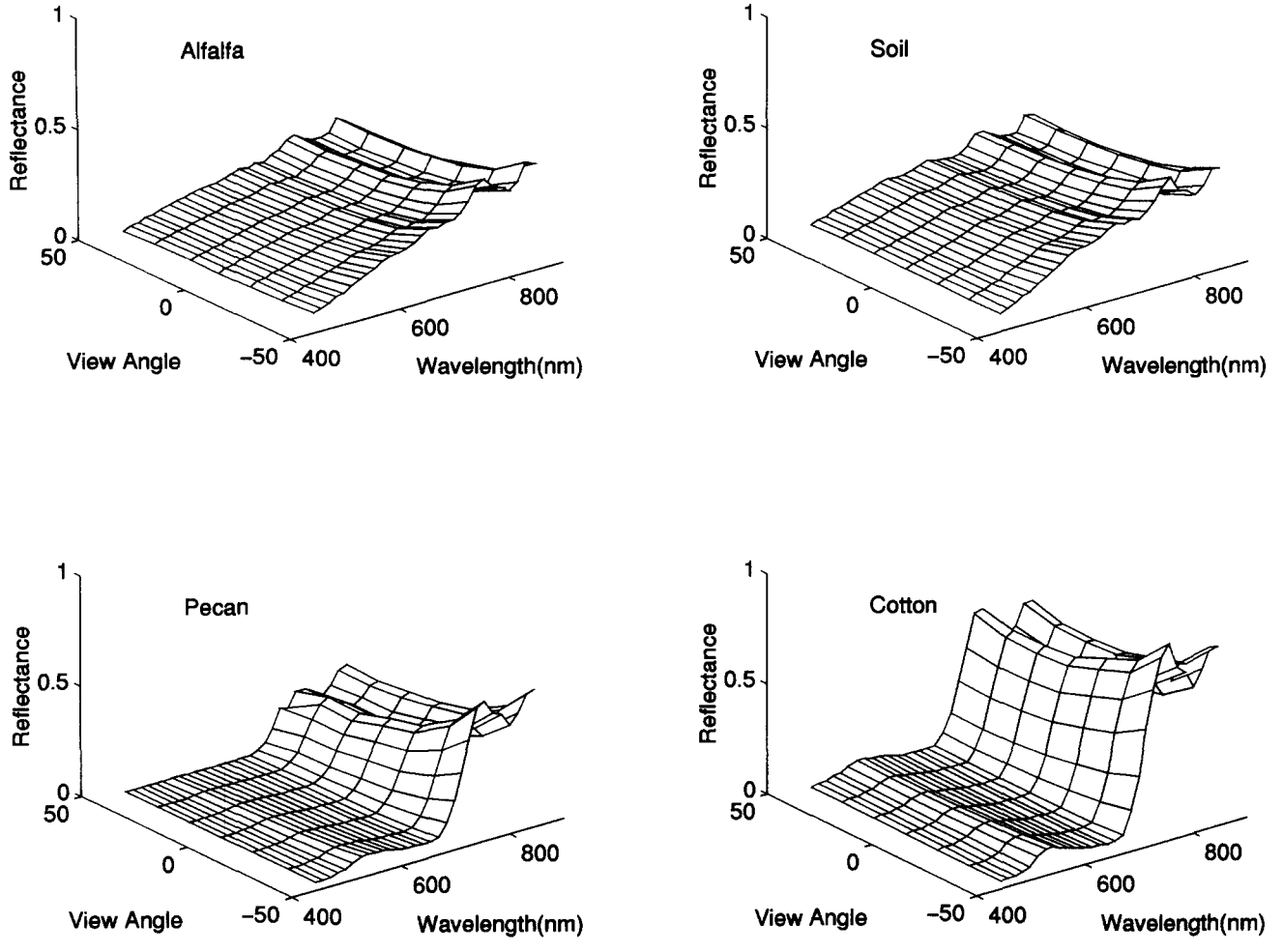

Figure 4. Three dimensional plots of the surface reflectances versus view angle and wavelength as measured with the ASAS sensor for harvested alfalfa (a), soil (b), pecan (c), and cotton (d) study sites at ~64° solar zenith angle.

lines), XS2 (dashed lines), and XS3 (dotted lines) spectral bands. The albedos were only a function of the solar zenith angles, increasing with solar zenith angles for alfalfa, cotton, and pecan sites, with exception of the soil site where the albedos of all three spectral bands slightly decreased at large solar zenith angles. By definition, the spectral albedos are void of view angles effect while the spectral reflectances (Fig. 4) or spectral reflectance-based vegetation indices (Fig. 5) were dependent on sun / view geometry. The spectral albedos of the red (XS2) waveband were "brighter" than those of the green (XS1) waveband for the alfalfa and soil sites (Figs. 6a and 6b), which indicated a yellowish appearance of these two sites. In contrast, the pecan and cotton (Figs. 6c and 6d) appeared green because of their high spectral albedos of the green waveband (XS1).

The NDVI values calculated with spectral albedos of the ASAS data are plotted in Figure 7 as a function of the solar zenith angles, along with those calculated with reflectances. The solid lines are the NDVI values computed with spectral albedos of 7 September data and the dashed lines are those computed from 8 September data. The stars (*) are the NDVI values calculated with spectral reflectances of 7 September and the crosses (+) are those of 8 September. The vertical variations of those data points were due to the sensor view angle changes while horizontal variations were due to the solar zenith angles.

The view effects seen with reflectance-based NDVI in Figure 5 disappeared with the albedo-based NDVI as shown with the ASAS data in Figure 7. The albedo-based NDVIs were generally lower than reflectance-based NDVIs for the alfalfa (Fig. 7a) and soil (Fig. 7b) sites. For the pecan (Fig. 7c) and cotton (Fig. 7d) sites, the albedo-based NDVIs were generally within the range of those reflectance-based NDVIs. The solar zenith angle effects on the albedo-based NDVIs were much smaller than those on the reflectance-based NDVI values for all sites. The albedo-based NDVIs decreased with solar zenith angles for the alfalfa and soil sites (Figs. 7a and 7b), but increased for the pecan and cotton sites (Figs. 7c and 7d). Considering that most measurements in practice

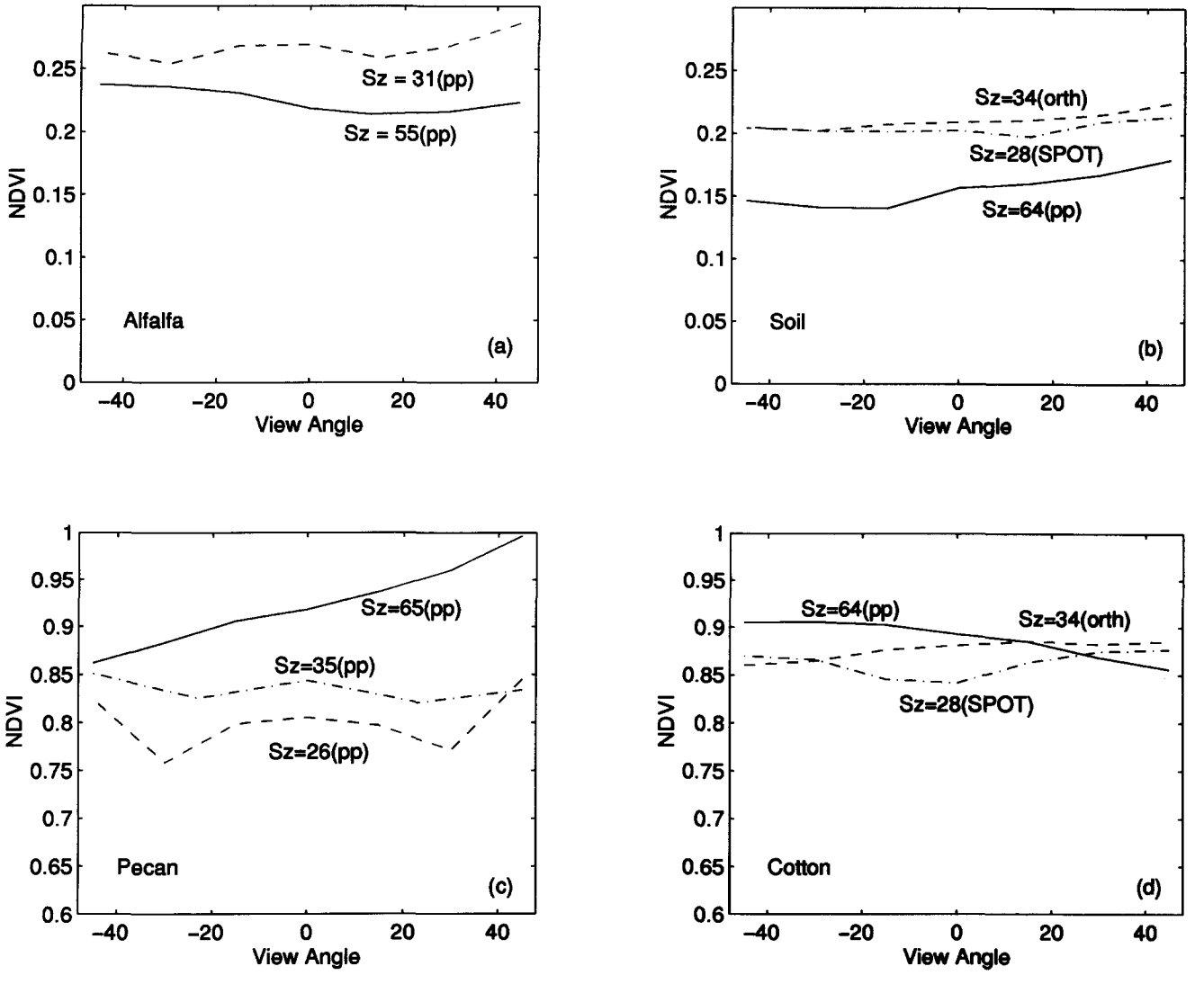

Figure 5. Sun / view angle effects at ground level on NDVI for alfalfa (a), soil (b), pecan (c), and cotton (d) study sites using the ASAS data. The solar zenith angle (S_z) angles are in degrees while the view directions are either in principal plane (pp), or orthogonal (orth) to pp, or in the SPOT view direction.

(satellite passes) occurred in the late morning (the solar zenith angles are probably less than 40°), the variations found with the albedo-based NDVIs are negligible. In comparison, the reflectance-based NDVI values varied not only with the solar positions, but also with the view angle magnitudes. At the alfalfa site (Fig. 7a), for example, the uncertainty (defined here as the difference between the maximum and minimum NDVI values) was 0.03 due to view angle differences, and 0.04 due to solar zenith angles, which added up to 0.07 in NDVI unit when both sun and view angles were considered. The uncertainty for the partially covered pecan orchards (Fig. 7c) was the worst (0.25) of all, which could be due to the heterogeneity of the pecan canopy. The large difference in reflectance-based NDVI values from one day to the next (7 and 8 September) could be due to the influence of view and sun angle variations. Take the absolute difference between the maximum and minimum NDVI values as an example. The variations in NDVI values from 7–8 September were 25%, 20%, and 12% for soil, pecan, and cotton targets, respectively. Since the vegetation changed little within the two consecutive days, the differences found with the reflectance-based NDVI were solely attributed to the sun and view angle effects. In contrast, the albedo-based NDVI variations between the two days were only 6%, 3%, and 1% for soil, pecan, and cotton targets at the corresponding sun angles of the two days.

The sun and view angle effects were also vegetation type dependent (Fig. 7) for the reflectance-based NDVIs. The sun angle effects were more pronounced than the view angle effects for less vegetated sites (alfalfa and bare soil), but the view angle effects exceeded the sun angle influences for the highly green-vegetation covered

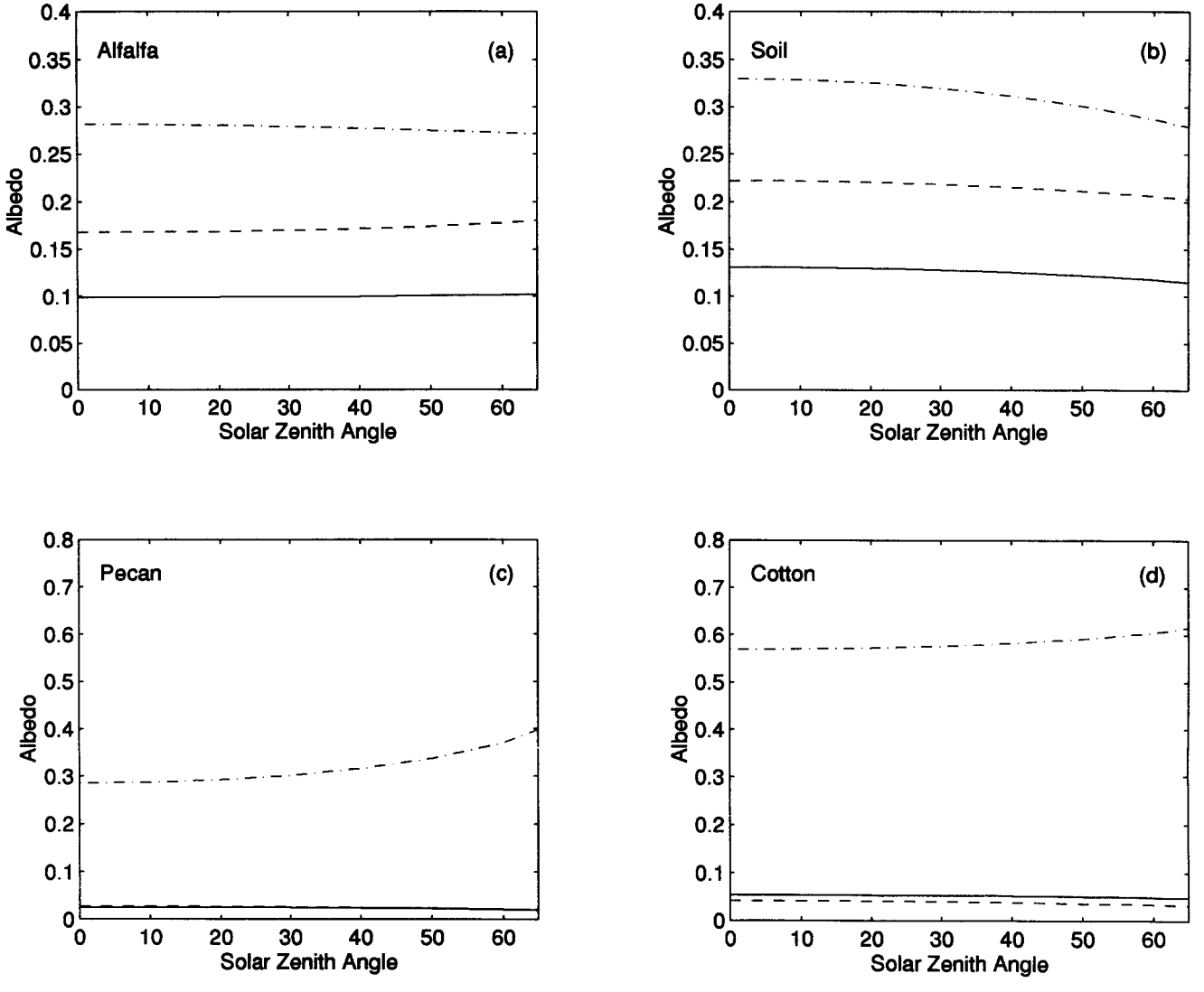

Figure 6. Spectral albedos calculated with simulated bidirectional reflectances for alfalfa (a), soil (b), pecan (c), and cotton (d) study sites using ASAS data. The solid lines are XS1, dashed lines are XS2, and the dotted lines are the XS3 bands.

sites (pecan and cotton). The dependency of the sun / view angle effects on surface type makes it impossible to properly interpret the reflectance-based NDVIs unless a prior knowledge about the surface is known. In contrast, the albedo-based NDVIs were void of the view angle effects and varied slightly with the sun angles. Because the possible range of the albedo-based NDVI values was the same as that of the reflectance-based NDVIs, albedo-based NDVIs would be equally sensitive to vegetation as the reflectance-based NDVIs.

The sun / view angle effects on both albedo- and reflectance-based NDVIs are further demonstrated with the aircraft and SPOT satellite data in Figure 8. Only cotton, pecan, and soil sites are shown because no aircraft data for the alfalfa site were available. The circles (O) and the "×" were the NDVIs computed with the SPOT reflectances of the two days. The albedo-based NDVIs (lines) varied little, going through those data points of reflectance-based NDVI. The sun angle effects on albedo-based NDVIs of the cotton (Fig. 8a) and soil (Fig. 8c) sites were much less than those of the pecan site (Fig. 8b), as indicated by almost invariant albedo-based NDVI lines. The largest discrepancies among the reflectance-based NDVIs were found with the pecan site (Fig. 8b), which were attributable again to the shadowing by the pecan trees. Differences were also found between the NDVI values computed from the data acquired with different sensors (SPOT, ASAS, and aircraft). The NDVIs from SPOT data were about 15% lower than those from aircraft measurements for cotton and pecan sites, and about 2% higher for the soil site. Several factors could have caused these discrepancies; one is the atmospheric effects, although corrections were made, and another is the radiometric calibration of the sensors.

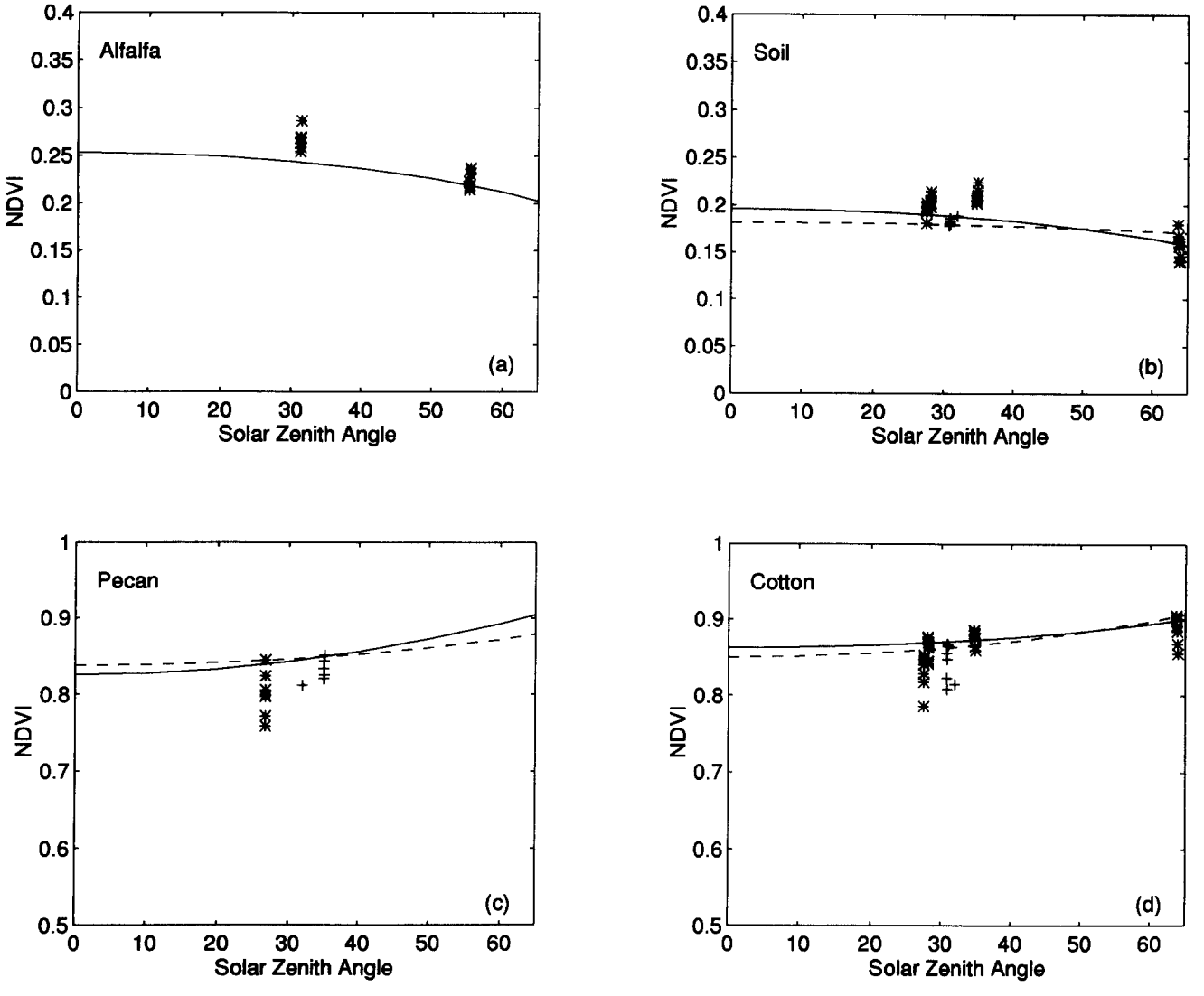

Figure 7. The NDVI values of alfalfa (a), soil (b), pecan (c), and cotton (d) study sites computed from spectral albedos (lines). The stars (*) and crosses (+) are the NDVI values calculated from spectral reflectances collected on DOYs 250 and 251, respectively.

DISCUSSION AND CONCLUSIONS

The view angle effects on the spectral reflectances were inherent in the reflectance-based NDVIs, but they disappeared in albedo-based NDVI calculations. The computation of the spectral albedo-based vegetation indices required simultaneous multidirectional measurements over the same targets, and, therefore, the spectral albedo computation was dependent on the number of input measurements. The stability of the spectral albedos as a function of the number of the input measurements is illustrated in Figure 9. When the number of the input measurements was small, the calculated albedos varied substantially. With the increase in the number of measurements, however, the albedo gradually became constant. The minimum number of input measurements in this study was seven for cotton site and nine for soil site. In practice, we usually do not have simultaneous multidirectional measurements, and, therefore, the application of this albedo-based vegetation index would be limited. However, this limitation can be tackled in several ways. One method would be to use measurements of different sensing systems such as the SPOT, Thematic Mapper, and the AVHRR (Moran et al., 1994). In this case, the data obtained with different sensors would be well cross-calibrated, and the surfaces of study ought to be homogeneous. Another option would be to use high frequency multitemporal measurements. Within a short period of time (a few days), vegetation can be assumed to change little, and the measurements made within that time period can be treated as if the data were collected at the same time, but with different sun / view configurations. Considering that the albedo-based vegetation indices were so much more independent of the view angle effects than the reflectance-based

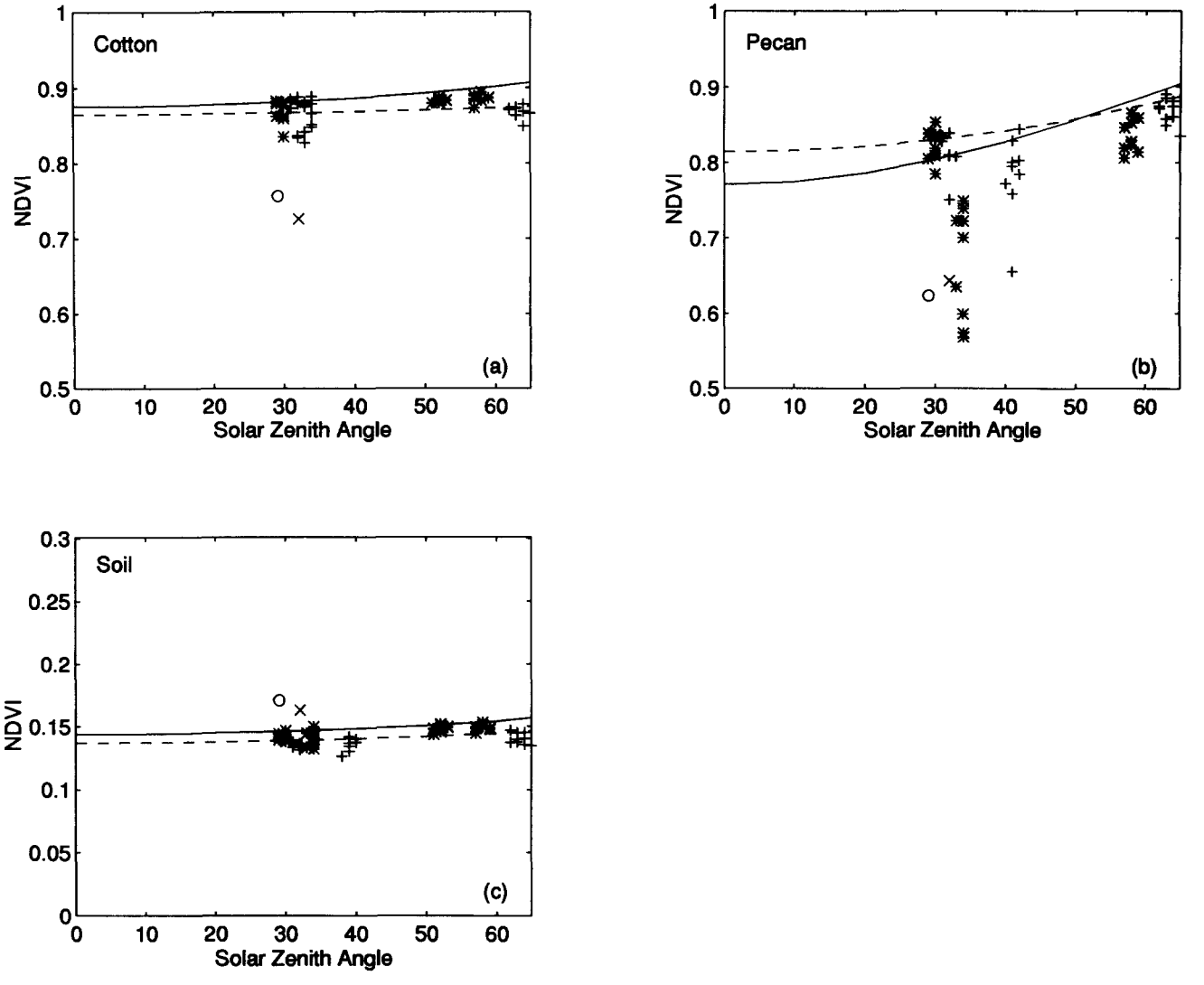

Figure 8. Same as Figure 7, except that the data used were aircraft (*) and SPOT acquired on 7 (×) and 8 (O) September.

NDVIs, obtaining extra measurements appears justified, providing a meaningful way to compare data across time and space for vegetation monitoring.

Although promising, the albedo-based vegetation indices may not be suitable for large images, because substantial inversion and simulation time is needed. This problem can be tackled by employing simple BRDF models using faster computers, or by using advanced processing techniques. The latter method needs more investigation.

The albedo-based vegetation index is dependent upon the performance of the selected BRDF models, because the albedo calculation was achieved with simulated data. Consequently, the selection or development of a simple, but accurate model might be crucial. Existing BRDF models have been found to be somewhat vegetation type dependent (Cabot et al., 1994), but most of them are equivalent in representing the surface bidirectional reflectance patterns. Some models, especially those which are physically based, require a large number of input parameters, and, therefore, more multidirectional remote sensing measurements are needed to invert them. In this case, the BRDF models with fewer required input parameters are preferable. On the other hand, simple empirical models may result in losses in accuracy because these models may not be well representative of the real world. Nevertheless, the albedo-based NDVI algorithm needs to be further investigated with other BRDF models, as well as with other data sets.

The albedo-based NDVI values varied slightly with the solar zenith angles, and it appeared that the variations were vegetation-type dependent. Therefore, a sensitivity study is needed to quantify the solar angle effects on the albedo-based indices, so that measurements made at different times and locations can be compared and

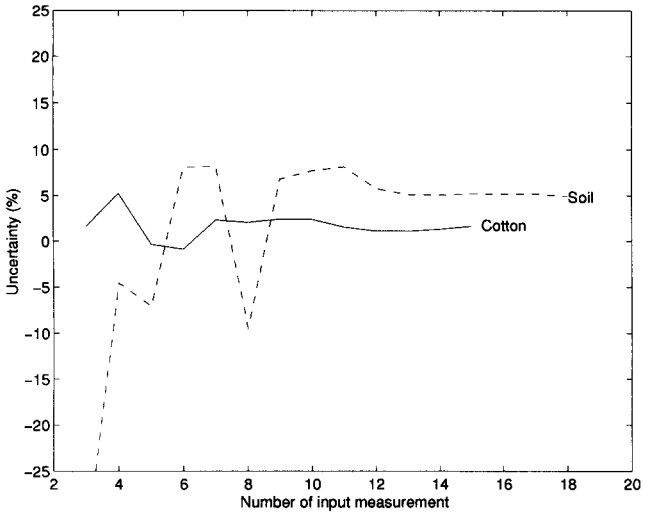

Figure 9. The dependency of the uncertainty in the spectral albedo calculation on the number of input measurements for soil (dashed line) and cotton (solid line) sites.

properly interpreted. It should also be pointed out, however, that if one could restrict the measurements to time when the absolute solar zenith angle is less than 40°, the sun angle effect should be very small, and may be neglected for some surface types.

Only view angle effects were normalized with the albedo-based vegetation indices in this study. There are many other external factors such as soil background variations and atmospheric conditions that influence reflectance-based vegetation indices (Qi et al., 1994b). To reduce these influences, other vegetation indices that prove to be less sensitive to soil and atmosphere conditions should be calculated with spectral albedos when necessary spectral bands (e.g., blue) are available. In this study, only the NDVI was tested, and the validity of other vegetation indices remains to be done. Finally, the albedo-based NDVI was only tested for bidirectional effects. Its sensitivity to vegetation type and to biophysical parameters, such as leaf area index, need to be further investigated. In conclusion, the bidirectional effects found with both reflectances and reflectance-based vegetation indices were normalized with the albedo-based indices, and, therefore, it is possible to compare remotely sensed data across time and space scales for farm management and environmental change studies.

The authors wish to acknowledge the Canadian Center for Remote Sensing and the USDA-Water Conservation Laboratory for the organization of the MAC-VI experiment. The authors wish to acknowledge Dr. Alfredo Huete (University of Arizona), Dr. Ghani Chehbouni (ORSTOM), Wim van Leeuwen (University of Arizona), and Ginger Paige (USDA-ARS Southwest Watershed Research Center) for their critical reviews and discussions. The authors wish to acknowledge Dr. Christoph Borel, Los Alamos National Laboratory Space Science and Technology for providing leaf area index data for the cotton field. The leaf area index data for the pecan field were obtained from the report "Field measurements with Li-Cor LAI-2000 at Maricopa" by Dr. John Miller (York University, Canada) and Dr. Ruiliang Pu (Nanjing Forest University, China) in THE MAC VI EXPERIMENT, *Maricopa, Arizona. The authors are grateful to the MAC staffs for providing study sites and for their assistance in field work.*

REFERENCES

Albuelgasim, A. A., and Strahler, A. H. (1994). Modeling bidirectional radiance measurements collected by the Advanced Solid-state Array Spectroradiometer over Oregon transect conifer forests, *Remote Sens. Environ.* 47:261–275.

Asrar, G., and Myneni, R. B. (1991), Applications of radiative transfer models for remote sensing of vegetation conditions and states, in *Photon–Vegetation Interactions, Applications in Optical Remote Sensing and Plant Ecology* (R. B. Myneni and Ross, Eds.), Springer-Verlag, New York, pp. 537–558.

Cabot, F., Qi, J., Moran, M. S., and Dedieu, G. (1994). Test of surface bidirectional reflectance models with surface measurements: results and consequences for the use of remotely sensed data, in *6th International Symposium on Physical Measurements and Signatures in Remote Sensing,* Val d'Isere, France, 17–24 January.

Cihlar, J., Manak, D., and Voisin, N. (1994), AVHRR bidirectional reflectance effects and compositing, *Remote Sens. Environ.* 48:77–88.

Deering, D. W., Eck, T. F., and Otterman, J. (1990), Bidirectional reflectances of selected desert surfaces and their three-parameter soil characterization. *Agric. For. Meteorol.* 52:71–93.

Gutman, G. G. (1991), Vegetation indices from AVHRR: an update and future prospects? *Remote Sens. Environ.* 35: 121–136.

Herman, B. M., and Browning, S. R. (1965), A numerical solution to the equation of radiative transfer, *J. Atmos. Sci.* 22:59–66.

Holben, B., and Kimes, D. (1986), Directional reflectance response in AVHRR red and near-IR bands for three cover types and varying atmospheric conditions, *Remote Sens. Environ.* 19:213–236.

Huete, A. R., Hua, G., Qi, J., Chehbouni, A., and van Leeuwen, W. J. D. (1992), Normalization of multidirectional red and NIR reflectances with the SAVI, *Remote Sens. Environ.* 41: 143–154.

Jackson, R. D., Teillet, P. M., Slater, P. N., et al. (1990), Bidirectional measurements of surface reflectance for view angle corrections of oblique imagery, *Remote Sens. Environ.* 32:189–202.

Liang, S., and Strahler, A. H. (1994), Retrieval of surface BRDF and albedo from multiangle remotely sensed data, *Remote Sens. Environ.* 50:18–30.

Moran, M. S., Jackson, R. D., Clarke, T. R., et al. (1995), Reflectance factor retrieval from Landsat and SPOT HRV data for bright and dark targets, *Remote Sens. Environ.*, 52: 218–230.

Mouginis-Mark, P. J., Garbeil, H., and Flament, P. (1994), Effects of viewing geometry on AVHRR observations of volcanic thermal anomalies, *Remote Sens. Environ.* 48:51–60.

Qi, J., Huete, A. R., Cabot, F., and Chehbouni, A. (1994a), Bidirectional properties and utilizations of high resolution spectra from a semi-arid watershed, *Water Resources Res.* 30(5):1271–1279.

Qi, J., Kerr, Y., and Chehbouni, A. (1994b), External factor consideration in vegetation index development, in *6th International Symposium on Physical Measurements and Signatures in Remote Sensing*, Val d'Isere, France, 17–24 January.

Qin, W. (1993), Modeling bidirectional reflectance of multicomponent vegetation canopies, *Remote Sens. Environ.* 46: 235–245.

Rahman, H., and Dedieu, G. (1994), SMAC: a simplified method for the atmospheric correction of satellite measurements in the solar spectrum, *Int. J. Remote Sens.* 15(1): 123–143.

Rahman, H., Pinty, B., and Verstraete, M. M. (1993a), A coupled surface-atmosphere reflectance (CSAR) model. Part 1: model description and inversion on synthetic data, *J. Geophys. Res.* 98:20,779–20,789.

Rahman, H., Verstraete, M. M., and Pinty, B. (1993b), A coupled surface-atmosphere reflectance (CSAR) model. Part 2: Semiempirical model usable with NOAA Advanced Very High Resolution Radiometer data, *J. Geophys. Res.* 98:20,791–20,801.

Schaaf, C. B., and Strahler, A. H. (1994), Validation of bidirectional and hemispherical reflectances from a geometric-optical model using ASAS imagery and Pyranometer measurements of a spruce forest, *Remote Sens. Environ.* 49: 138–144.

Strahler, A. H. (1994), Measuring and modeling the bidirectional reflectance of plant canopies, in *6th International Symposium on Physical Measurements and Signatures in Remote Sensing*, Val d'Isere, France, 17–24 January.

Strahler, A. H., and Jupp, D. L. B. (1991), Geometric-optical modeling of forests as remotely-sensed scenes composed of three-dimensional, discrete objects, in *Photon–Vegetation Interactions, Applications in Optical Remote Sensing and Plant Ecology* (R. B. Myneni and Ross, Eds.), Springer-Verlag, New York, pp. 415–440.

Tanré, D., Deroo, C., and Duhaut, P., et al. (1990), Description of a computer code to simulate the satellite signal in the solar spectrum: the 5S code. *Int. J. Remote Sens.* 11(4): 659–668.

Verhoef, W. (1984), Light scattering by leaf layers with application to canopy reflectance modeling, the SAIL model, *Remote Sens. Environ.* 16:125–141.

Verstraete, M. M., Pinty, B., and Dickinson, R. E. (1990), A physical model of the bidirectional reflectance of vegetation canopies, 1: Theory, *J. Geophys. Res.* 95:11,755–11,765.